539886

NASA Cosmochemistry Grant NAG5-7285 Final Report
Mineralogy and microstructures of chock-induced melt veins in chondrites

Thomas G. Sharp

Grant period 5/1/98 – 4/30/00

1. Introduction

Shock metamorphism results from high-velocity collisions on planetary bodies and therefore represents a fundamental process in the formation of meteorites as well as the accretion and modification of planetary bodies in the solar system. The metamorphic effects of shock on meteorite samples such as deformation, brecciation, local melting and phase transformations, provide essential records of impact processes that can be investigated in a large number and variety of samples. Understanding shock effects on primary features in meteorites remains an important reason for further detailed studies of shock metamorphic processes in meteorites.

Shock metamorphic features and shock-induced melt veins have been the study of many investigations since (Fredriksson et al. 1963) interpreted black veins as shock-induced melt. The veins form by localized melting and commonly contain large polycrystalline clasts of high-pressure minerals such as ringwoodite and majorite surrounded in a matrix of very fine-grained high-pressure minerals that crystallized from the melt at high pressure (Chen et al. 1996). In our initial work of melt veins in Sixiangkou (L6, S6) (Chen et al. 1996; Chen et al. 1996; Sharp et al. 1996), we discovered a melt-vein assemblage consisting of magnesiowüstite plus majorite. This assemblage, which is the stable liquidus assemblage observed in experiments from approximately 23 to 25 GPa and 2000 °C (Agee et al. 1995), allowed us to estimate crystallization pressures and temperatures for the first time. This provided the first evidence that melt-vein assemblages could be similar to those of a static high-pressure experiments (Sharp et al. 1995; Chen et al. 1996; Chen et al. 1996; Chen et al. 1996; Sharp et al. 1996; Sharp et al. 1996). The applicability of phase equilibrium data to the interpretation of shock-induced melt veins can only be tested by a detailed study of melt-vein mineralogy to see how high-pressure assemblages vary as a function of shock conditions inferred from other indicators. We have used transmission electron microscopy (TEM), analytical electron microscopy (AEM), scanning electron microscopy (SEM), electron microprobe analysis (EMA) and optical petrography to characterize the mineralogy, microstructures, and compositions of melt veins and associated high-pressure minerals in shocked chondrites and SNC meteorites. In the processes, we have gained a better understanding of what melt veining can tell us about shock conditions and we have discovered new mineral phases in chondritic and SNC meteorites

2. Proposed Research Objectives

The primary objective of this research was to use microstructural and microanalytical techniques to characterize shock-induced melt veins and associated high-pressure minerals that occur in chondritic meteorites ranging from S3 to S6 shock stages. The data was intended to provide a better understanding of the formation and crystallization of melt veins and the transformation mechanisms and kinetics of associated forming high-pressure minerals.

A) Look at mineralogy and microstructures of melt-veins in a suite of L4 through L6 chondrites ranging from shock grades S3 through S6 to determine how crystallization and assemblages are controlled by intensity of shock metamorphism.

B) Investigate the chemical, mineralogical, and microstructural heterogeneities within melt veins to elucidate the extent of melt-mixing and the range of crystallization processes in melt veins and pockets.

C) Use static high-pressure experiments to produce examples of equilibrium and quench crystallization for comparisons with the melt veins of naturally shocked samples using transmission electron microscopy (TEM) and scanning electron microscopy (SEM).

D) Characterize the mineralogies, compositions, and defect microstructures of polycrystalline aggregates of ringwoodite, wadsleyite, and majorite associated with melt veins in S6 samples. The microstructural and microanalytical data will be used to understand the mechanisms and kinetics of phase transformations that occur during shock metamorphism of chondrites.

E) We will investigate the extent of back transformations of metastable high-pressure minerals to better understand the thermal histories of samples after shock release. This information will be interpreted in terms of post-shock cooling histories and the relation between post-shock heating and peak-shock pressures.

Our actual research results deviate somewhat from those proposed because of some very important research that we conducted on new SiO_2 minerals in Shergotty. Our research results for the grant period are summarized below and published scientific papers are attached.

3. Results

Melt-vein mineralogy and microstructure vs. shock stage

Although shock-induced deformation and transformation features have been used to classify chondrites by shock stage (S1–S6) and provide an estimate of shock pressures (Stöffler et al. 1991), the conditions required to form high-pressure minerals are not well understood. Shock-induced melt veins, common in L5 and L6 chondrites, contain high-pressure mineral assemblages that can constrain crystallization conditions that occurred during shock (Stöffler et al. 1991; Chen et al. 1996; Sharp et al. 1997). Melt vein assemblages may provide an alternative shock-pressure calibration, depending on when melt veins crystallize during shock events. We have examined 11 melt-vein-bearing L chondrites that range from shock stage S3 to S6 to determine how melt-vein texture and mineralogy correlate with the shock stage. These samples include: Roy, La Landa, Gifu, Umbarger, Waconda, Pinto Mountains, Beaver, Kunashak, Nakhon Pathon, Tenham, and Ramsdorf. Shock effects in olivine and plagioclase were characterized petrographically to determine the shock stage. Black veins were characterized by optical microscopy, Field-emission scanning electron microscopy (FESEM), Raman spectroscopy and transmission electron microscopy (TEM). Qualitative microanalyses of the melt-vein minerals were obtained using energy dispersive X-ray spectroscopy (EDS) combined with both FESEM and TEM.

Nine of the samples were previously classified as S3 though S6 (Stöffler et al. 1991). We find that the shock stages for most of these samples agree with the previous grade determination if we ignore the transformation features that occur in or adjacent to melt veins. However, considering transformation effects associated with melt veins, we find that three of the samples contain evidence for higher shock stages. Roy, previously classified as S3 (Stöffler et al. 1991), contains well-developed maskelynite around melt veins suggesting S5. Ramsdorf, previously classified as S4 (Stöffler et al. 1991), and S6 (Yamaguchi et al. 1996) shows strong mosaicism in olivine and the presence of maskelynite near melt veins suggesting S5. Umbarger, previously classified as S4 (Stöffler et. al 1991), contains well-developed maskelynite and shock-melted plagioclase near melt veins as well as deep-blue ringwoodite in melt pockets. Based on Stöffler's classification, Umbarger is S6. The remaining samples are S4 (La Landa, Gifu, Waconda, Kunashak, and Nakhon Pathon,), S5 (Beaver, Pinto Mountains and Ramsdorf) and S6 (Tenham).

Textural variations

Low-grade veins: Roy (S3), Gifu (S4), and Nakhon Pathon (S4) have melt-veins that are dominated by metal-sulfide surrounding angular silicate fragments. These small silicate grains (< 500 nm to > 50 μm) suggest that melt-vein formation involved

cataclasis and frictional melting of metal sulfide. Roy contains evidence for multiple veining events, with one vein showing evidence for both silicate and metal-sulfide melts.

Intermediate-grade veins: Kunashak (S4), La Landa (S4) and Ramsdorf (S5) all have very similar melt veins that are predominantly silicate with irregularly shaped blebs and rounded droplets of metal-sulfide. The irregular shapes suggest of the metal-sulfide liquid in the veins was in contact with solid-silicate grains in a partially molten silicate matrix. Rounded metal-sulfide droplets indicate immiscible metal-sulfide and silicate liquids.

High-grade veins: Umbarger (S6) and Tenham (S6) contain melt veins and pockets with predominantly round metal-sulfide droplets in a silicate matrix, indicating immiscible metal-sulfide and silicate liquids. However, variations in the proportions of silicate to metal-sulfide liquids suggest multiple veining events. The habits of the silicate gains vary from vein rims to cores in both samples. Cores have granular textures whereas the vein margins have acicular textures suggestive of a quenched margin.

High-pressure minerals in melt veins

Roy: The small amount of silicate melt in Roy (S3) crystallized to for an assemblage of ringwoodite plus majorite. Based on the phase diagram of Allende (Agee et al. 1995)this represents near liquidus crystallization between about 18 and 23 GPa. These conditions are similar to those found in S6 samples.

Ramsdorf: The silicate melt in Ramsdorf (S4) contains glass and clinoenstatite. The clinoenstatite shows no evidence of twinning and is probably the high-pressure form, which is stable up to about 16 GPa in enstatite-forsterite system. This assemblage indicates rapid quench and crystallization between about 10 and 16 GPa.

Umbarger: Umbarger contains both high-pressure lithologies. The melt veins and pockets contain many (10 to 50 μm) grains of polycrystalline ringwoodite that represent transformation from olivine at pressure in excess of 16 GPa and possibly much higher. Apparent maskelynite that occurs adjacent to melt veins is actually polycrystalline material with the hollandite structure. The melt-vein matrix contains akimotoite ($(Mg,Fe)SiO_3$-ilmenite), ringwoodite and augite where augite is clearly the last mineral to crystallize. Because akimotoite is not a liquidus phase in chondritic or peridotitic compositions, its occurrence suggests large supercooling. The sequence of crystallization suggests a pressure decrease from 18-25 GPa to < 18 GPa with supercooling.

Tenham: Tenham also contains both high-pressure lithologies. The polycrystaline lithogy includes ringwoodite, majorite, akimotoite and $(Mg,Fe)SiO_3$-perovskite (Tomioka and Fujino 1997). These polycrystalline phases represent phase transitions at pressures in excess of 22 GPa and possibly much higher. The melt-vein matrix contains assemblages that include akimotoite plus ringwoodite at melt vein margins, majorite plus magnesiowüstite (and magnetite) as the predominant assemblage and majorite plus ringwoodite in some core regions. These assemblages correspond to crystallization of most of the veins at 23 – 25 GPa, but with super cooling of the margins between 18 and

25 GPa. The majorite-plus-ringwoodite assemblage records a lower pressure (18-23 GPa) in some melt vein cores.

The textures of melt veins vary systematically as a function of shock grade. The melt veins in Roy reached temperatures > 950 °C, sufficient to melt the Fe-Ni-metal-sulfide, but only a small amount of silicate was melted. The cataclastic textures of sulfide-rich veins indicates mechanical mixing of silicate components and frictional heating to produce mixed silicate and sulfide melt veins. The intermediate and high-grade veins reached significantly higher temperatures, resulting in more silicate melting. Variations in mineral habits across melt veins suggest variable thermal histories for the different parts of the melt veins.

Although the melt-vein mineralogy is useful in constraining the pressure temperature conditions of crystallization, there is considerable debate about the relationship between crystallization pressure and the equilibrium shock pressure. If a melt vein cools through the liquidus during the period of equilibrium shock pressure, a melt-vein or pocket should contain one assemblage corresponding to that pressure. If melt veins in various samples crystallized at the equilibrium shock pressure, melt-vein assemblages should vary systematically with shock stage. However, if crystallization of melt veins occurs during adiabatic decompression, a range of crystallization pressures would be recorded in a single sample and there should be no systematic variation of melt-vain mineralogy with shock grade. There does not seem to be a systematic variation in the crystallization pressures with shock stage in the samples studied here. For example, Roy (S3) contains majorite plus ringwoodite (18-23 GPa) that also occurs in Tenham whereas Ramsdorf (S4) contains a lower-pressure assemblage (10-16 GPa). Both Umbarger and Tenham contain evidence for varying crystallization pressures within single melt veins. The melt-vein assemblage in Umbarger is consistent with disequilibrium crystallization during rapid cooling and decompression with crystallization starting as high has 25 GPa and ending below 18 GPa. The melt-vein assemblages in Tenham are dominated by the liquidus assemblage of majorite plus magnesiowüstite (23-25 GPa), whereas the margins are represent supercooling at similar pressures (18-25 GPa). The majorite-plus-ringwoodite assemblage represents near liquidus crystallization at lower pressure (18-23 GPa), indicating that at least some of the crystallization was accompanied by decompression.

Pressure Constraints from the Survival of Metastable Phases

Because melt-vein crystallization pressures may be lower than equilibrium shock pressure, we need additional methods of constraining the equilibrium shock pressure. The post-shock temperature of a given sample, which is related to equilibrium shock pressures, can be constrained by the survival of metastable minerals. Phases such as $MgSiO_3$-perovskite, $MgSiO_3$-ilmenite are unable to survive high temperatures at low

pressure so they are sensitive to post-shock temperatures. At one atmosphere, $MgSiO_3$-perovskite and akimotoite ($MgSiO_3$-ilmenite) vitrify at approximately 750 K and 973 K, respectively. The Tenham L6 chondrite, which contains akimotoite and $MgSiO_3$-perovskite, is unlikely to have experienced post-shock temperatures above 750 K. The Acfer 040 L5-6 chondrite, which contains $(Mg,Fe)SiO_3$-ilmenite and vitrified $(Mg,Fe)SiO_3$-perovskite, experienced a post-shock temperature less than 973 K, but greater than 750 K. Based on the calibration of equilibrium shock pressure and estimates of post-shock temperature (Stöffler et al. 1991), Tenham experienced an equilibrium shock pressure less than about 40 GPa, which is consistent with the maximum crystallization pressures of 25 GPa, based on melt-vein assemblages. Acfer 040 appears to have experienced an equilibrium shock pressure less than 48 GPa. In this case, akimotoite and $(Mg,Fe)SiO_3$-perovskite crystallized from the melt-vein liquid at a pressure above about 18 GPa to well over 25 GPa. The Perovskite-akimotoite-ringwoodite assemblage indicates crystallization during rapid cooling and decompression. Because the metastable minerals occur in the hottest part off the sample (the melt-vein), the pressure constraint provided by the survival of metastable minerals may be significantly higher than the actual equilibrium shock pressure. Pressure constraints from survival of metastable phases and from crystallization suggest equilibrium shock pressures that are lower than those based on the pressure calibration of (Stöffler et al. 1991).

Hollandite-structured maskelynite

Maskelynite is an optically amorphous form of shocked plagioclase that is generally considered to be a diaplectic glass. In highly shocked samples there is commonly evidence of flow (Stöffler et al. 1991; El Goresy et al. 1997). which suggests that some plagioclase vitrifies through melting rather than through pressure-induced amorphization. Such melted material has been used to argue that "maskelynite" is not diaplectic glass (El Goresy et al. 1997). Crystalline "maskelynite" with the hollandite structure has been discovered in the L6 chondrites Sixiangkou (Gillet et al. 2000) and in Tenham (Tomioka et al. 1999). In one case, the material was characterized by Raman and X-ray diffraction (Gillet et al. 2000) while in the other (Tomioka et al. 1999), TEM was used. We used TEM to characterize the microstructures of the hollandite-structured plagioclase in Sixiangkou and Tenham in order to constrain the origins of this new high-pressure mineral.

Electron imaging and diffraction of the maskelynite near a melt vein in Sixiangkou show that the maskelynite that occurs more than about 100 μm from the melt vein is completely amorphous on a nanometer scale. However, maskelynites adjacent to and within melt veins in both Sixiangkou and Tenham are full of crystals, ranging from 20 to 70 nm, that occur in an amorphous matrix (Fig. 1). These crystals are regular in shape

and randomly oriented. These crystals are beam sensitive and readily vitrify during TEM imaging at high magnification. This semi-crystalline maskelynite occurs both in large grains and within melt veins (Fig. 1). The vein filling morphology indicated that some of this material was liquid at the time of vein formation.

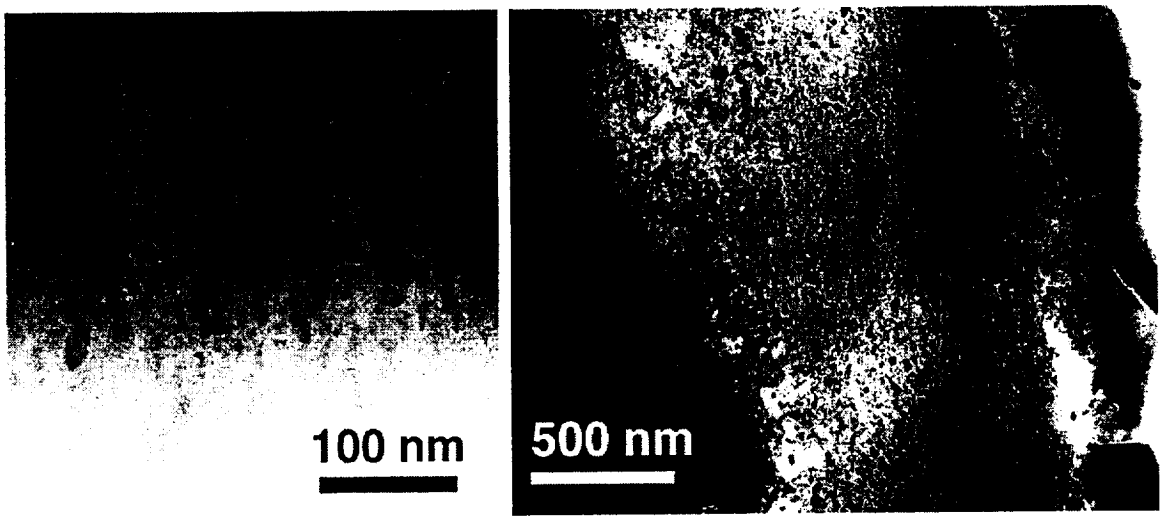

Figure 2. HRTEM image of nanocrystalline hollandite (left) in an amorphous matrix from Tenham. Bright field image (right0 showing a vein of hollandite structured plagioclase in Tenham.

Selected-area electron diffraction patterns consist of spotty rings made up of many Bragg reflections (Fig. 2). The quality of the ring patterns indicates that the crystallites are randomly oriented and very small. The patterns consist of up to 12 rings, all of which can be indexed, within error (≈ 5%), as the hollandite structure. The observed d-spacings match calculated d-spacings for hollandite, using the unit cell parameters of (Gillet et al. 2000). For Sixiangkou, 11 out of 12 rings are definitively indexed, with the remaining ring being within error of two of the calculated d-spacings (510 and 411). For Tenham, 8 out of 10 rings are definitively indexed with the remaining two rings being within error of two d-spacings each (240, 310) and (321, 510). Although indexing of one or two closely spaced lines is problematic, the fit of the remaining diffraction rings confirms that this nanocrystalline material has the hollandite structure.

Figure 2 SAED pattern of hollandite structured plagioclase in Sixiankou.

Qualitative EDS measurements on the TEM from Sixiangkou are consistent with this material being an albite-rich plagioclase with a minor orthoclase component. This is in agreement with electron microprobe analyses of the maskelynite in Sixiangkou ($Ab_{80}An_{12}Or_8$) and in Tenham ($Ab_{75}An_{15}Or_{10}$).

The fact that the hollandite-structured maskelynite only occurs very near melt veins, indicates that the transformation of plagioclase to the hollandite structure requires high temperatures. Based on the majorite-magnesiowüstite assemblage in the melt veins of Sixiangkou (Chen et al. 1996) the melt veins crystallized at approximately 2000 °C. The very similar matrix assemblage in Tenham indicates similar crystallization conditions. As in other high-pressure transformations in shocked chondrites, high temperatures are required for the reaction kinetics to be fast enough for transformation on the short time scales of shock.

The origin of the mixed glassy and nanocrystalline hollandite may be the result of either partial crystallization of a high-density liquid or glass or the result of partial amorphization of the polycrystalline hollandite-structured plagioclase. The random orientations and regular rounded shapes of the hollandite crystallites are not consistent with partial amorphization of hollandite after pressure release. In such post-shock vitrification the high-pressure phase would likely be cut by veins of amorphous material, as in the post-shock amorphization of high-pressure SiO_2 polymorphs (Sharp et al. 1999). Such vitrification leaves crystalline remnants that commonly have identical or nearly identical orientations. The randomly oriented hollandite grains in an amorphous matrix suggests that the hollandite crystallized from either a glass or a liquid at high pressure.

Veins of plagioclase composition material with nanocrystalline hollandite (Fig. 2) indicate that at least some the hollandite crystallized from a liquid during shock. However, complete melting of plagioclase within and adjacent to melt veins, at the same time that the melt veins were liquid, is inconsistent with the sharp boundaries commonly observed between "maskelynite and melt vein matrix. The melting of plagioclase in and adjacent to melt veins may occur after the initial melting and partial solidification of the melt vein.

The presence of plagioclase with the hollandite structure is consistent with the lower pressure of the crystallization pressures of Sixiangkou and Tenahm (23 –25 GPa and 2000°C). Experimental studies of $NaAlSi_3O_8$ at high pressure (Liu 1978) indicate that the calcium ferrite structure plus stishovite, rather than hollandite, are stable above 23 GPa.

Post-stishovite SiO_2 polymorphs in Shergotty

Shock metamorphism is characterized by deformation microstructures and high-pressure minerals and glasses. Quartz is a important indicator of shock metamorphism

because it forms planar deformation features (PDFs) (Chao 1967; Gratz et al. 1988) and because it transforms into the high-density polymorphs such as coesite and stishovite (Chao et al. 1960; Chao et al. 1962; Chao 1967; Stöffler 1972; Stöffler and Langenhorst 1994). Experimental studies (German et al. 1973; Sekine et al. 1987; Tsuchida and Yagi 1989; Tsuchida and Yagi 1990; Kingma et al. 1995; Dubrovinsky et al. 1997) and theoretical studies (Tse et al. 1992; Belonoshko et al. 1996; Karki et al. 1997; Teter et al. 1998) of SiO_2 at high pressure have shown that there are structures more dense than stishovite, known as "post-stishovite" phases. Natural examples of dense SiO_2 phases were discovered in Shergotty and interpreted as "post-stishovite" structures that were produced during the shock metamorphism of Shergotty (El Goresy et al. 1998; El Goresy et al. 1998; Sharp et al. 1998). The dense SiO_2 was initially thought to have the α-PbO_2 structure (El Goresy et al. 1998), but subsequent diffraction experiments have shown more complex structures (El Goresy et al. 1998; El Goresy et al. 1998; Sharp et al. 1998; Sharp et al. 1999). Here we combine field-emission scanning electron microscopy (FESEM), powder X-ray diffraction (XRD), transmission electron microscopy (TEM), selected area electron diffraction (SAED) to characterize two new SiO_2 structures and discuss these polymorphs in terms of the shock pressure experienced by Shergotty.

Silica in Shergotty mostly occur as large (>150 μm) wedge-shaped grains typical of β-tridymite. They are embedded in clinopyroxene or between clinopyroxene, mesostacis, and "maskelynite". Each grain is surrounded by radiating cracks that initiate at the surfaces of the silica grains and penetrate deep (up to 600 μm) in the Shergotty matrix (Fig. 3a). The radiating cracks are similar to those reported from ultra-high pressure metamorphic rocks around coesite grains and are indicative of a large volume increase after decompression. The individual silica grains consist of mosaics of many domains (10-60 μm), many displaying an orthogonal intergrowth of two or more sets of lamellae with different brightness in back-scattered electron images (Fig. 3b). Electron microprobe analyses show that the lamellae and lamellae-free areas are almost pure SiO_2 with minor amounts of Na_2O (0.40 wt. %) and Al_2O_3 (1.14 wt. %). A 120 μm disc containing a large silica (> 60 μm) grain was cored out with a high-precision diamond micro-drill for successive X-ray and TEM investigation.

Our initial electron diffraction data fit a post-stishovite structure similar to α-PbO_2. Since the initial investigation we have obtained diffraction patterns from three distinct zone axes, providing seven diffraction vectors to constrain the structure of this SiO_2 polymorph (Table 1). The corresponding d-spacings cannot be indexed using any structures of low-pressure SiO_2 polymorphs, including tridymite. Similarly, the diffraction data are inconsistent with coesite, stishovite and the known post-stishovite structures: $CaCl_2$-type, baddelyite -type, modified baddelyite (SBAD) and α-PbO_2 structures. However, the data nearly fit a synthetic orthorhombic Pbcn structure (German

et al. 1973) and a calculated orthorhombic structure ($Pca2_1$) except for the 1.97 Å and 3.41 Å reflections.

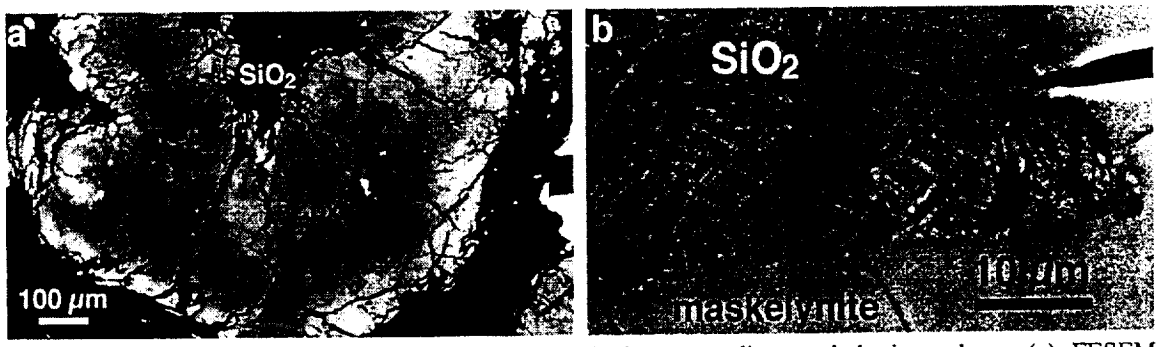

Figure 3. BSE images of SiO_2 showing radiating cracks in surrounding maskelynite and cpx, (a). FESEM BSE images (b), show a fine lamellae microstructure in the SiO_2 grains.

Since our diffraction patterns are consistent with orthorhombic symmetry, we used the Pbcn and $Pca2_1$ structures as starting points to refine new cell parameters and d-spacings (Table 1.). Our data fit the refined Pbcn and $Pca2_1$ unit cells in terms of d-spacings, pattern symmetry, interplanar angles and angles between zone axes. However, the systematic absences expected for the Pbcn structure provide the best match to the extinctions in our data. We conclude that the SiO_2 phase in Shergotty, initially described as α-PbO_2, (El Goresy et al. 1998), is a dense orthorhombic structure that fits the Pbcn space group and has cell parameters a = 4.17 Å, b = 5.12 Å and c = 4.55 Å and density $\rho = 4.18$ g/cm^3.

d-obs	Pbcn		$Pca2_1$		ref-Pbcn		ref-$Pca2_1$	
	hkl	d-calc	hkl	d-calc	hkl	d-calc	hkl	d-calc
4.54*	001*	4.50	100*	4.49	001*	4.55	100*	4.55
3.41*	011*	3.25	110	3.25	011*	3.40	110	3.40
3.22	110	3.17	011*	3.17	110	3.23	011*	3.23
3.09*	101*	3.11	101*	3.11	101*	3.07	101*	3.07
2.62	111	2.59	111	2.59	111	2.63	111	2.63
2.28	002	2.25	200	2.25	002	2.28	200	2.28
1.97	121	1.88	121	1.88	121	1.97	121	1.97

Table 1. Measured d-space data compared to calculated d-spacings for Pbcn, $Pca2_1$ and refined Pbcn, $Pca2_1$ unit cells. Extinct reflections which occur in diffraction patterns by double diffraction, are indicated by stars.

Powder X-ray diffraction data were collected from a single SiO_2 grain using a diffractometer with a rotating anode generator, capillary collimating system and CCD area detector. The beam was collimated to 0.1 mm diameter and focussed onto a single 60-μm SiO_2 grain. The diffracted X-rays were collected on a 512 x 512-pixel area

detector set at three fixed 2θ settings (15°, 25° and 30°). To make the relative intensities of the reflections more representative, the sample was rotated during data collection.

The silica grain contains amorphous material which produces a broad halo at 2θ = 8°-12°. A total of 18 reflections were collected from the silica grain (Table 2). Some of these (2.974(6), 2.023(4), 1.950(8), and 1.568(5) Å) belong to stishovite, but most of reflections could not be assigned to any known silica polymorph. A number of the observed reflections are close to reflections obtained from quenched α-PbO_2-like phase synthesized by (German et al. 1973), but several reflections (for example, 4.309(4), 2.767(3), 2.459) could not be indexed as the α-PbO_2-like structure. Instead we indexed all observed reflections (except a small broad reflection at 2.639(6)) in terms of a monoclinic lattice with the cell parameters a = 4.375(1) , b = 4.584(1), c = 4.708(1), β = 99.97(3), ρ = 4.30(2) g/cm^3. The density of this phase appears to be slightly higher than the density of stishovite (ρ = 4.28 g/cm^3, PDF #451374). The lattice parameters for the new phase are closely related to those of the baddeleyite - type structures. Moreover, 16 observed reflections of the new natural silica phase could be explained by the baddeleyite-type structure. Exceptions are the weak unindexed reflection at 2.639(6) and the reflection at 2.974(6), (which is forbidden for the baddeleyite structure). The latter reflection corresponds to the (110) reflection of stishovite (100% intensity reflection of stishovite). While quantitative analysis of the intensities of reflections of the new silica phase is difficult due to the strong preferred orientation and diffuse halo, the calculated intensities for SiO_2 with baddeleyite structure match the observed ones qualitatively very well (Table 2).

TEM and SAED investigations of the grain used for X-ray diffraction indicate the presence of the orthorhombic structure (Pbcn) described above, stishovite and an unidentified material that probably corresponds to the baddelyite-type structure. The three silica polymorphs are intergrown, forming a polymineralic grain. Some areas have a distinct lamellar microstructure with orthogonal crystalline lamellae (20-100 nm wide) cut by amorphous veins. Other regions are mostly amorphous with minor amounts of crystalline material. Amorphous veins occur throughout the SiO_2 and especially in the orthorhombic phase.

The presence of multiple SiO_2 structures is consistent with the complexity of post-stishovite SiO_2 phases (Belonoshko et al. 1996; Dubrovinsky et al. 1997; Karki et al. 1997; Teter et al. 1998). At P > 47 GPa, stishovite transforms to the $CaCl_2$ structure which transforms to a higher density-phase (α-PbO_2, modified α-PbO_2, or SBAD structures) at 70 to 80 GPa. A polyphase mixture of stishovite and other high-density SiO_2 structures in Shergotty is consistent with the fact that there are numerous post-stishovite structures that have very similar energies (Teter et al. 1998). One of which, the $CaCl_2$ structure, transforms to stishovite during quench. Similarly, the SBAD transforms

5. References

Agee, C. B., J. Li, et al. (1995). "Pressure-temperature phase diagram for the Allende meteorite." Journal of Geophysical Research **100**(B9): 17725-17740.

Belonoshko, A. B., L. S. Dubrovinsky, et al. (1996). "A new high-pressure silica phase obtained by molecular dynamics." American Mineralogist **81**((5-6)): 785-788.

Chao, E. C. T. (1967). "Shock effects in certain rock-forming minerals." Science **156**: 192-202.

Chao, E. C. T., J. J. Fahey, et al. (1962). "Stishovite, A new mineral from Meteor Crater, Arizona." Journal of Geophysical Research **67**: 419-421.

Chao, E. C. T., E. M. Shoemaker, et al. (1960). "First natural occurrence of coesite." Science **132**: 220-222.

Chen, M., T. G. Sharp, et al. (1996). "The high-pressure assemblage majorite-pyrope solid solution + magnesiowüstite: A new constraint on the high pressure and temperature history of shock melt veins in chondrites." LPS **XXVII**: 211-212.

Chen, M., T. G. Sharp, et al. (1996). "The majorite-pyrope + magneseowüstite assemblage: contraints on the history of shock veins in chondrites." Science **271**: 1570-1573.

Chen, M., B. Wopenka, et al. (1996). "High-pressure assemblages in shock melt veins in the Peace River (L6) chondrite: Compositions and pressure-temperature history." Meteoritics **31**: A27.

Dubrovinsky, L. S., S. K. Saxena, et al. (1997). "Experimental and theoretical identification of a new high-pressure phase of silica." Nature **388**(24 July): 362-365.

El Goresy, A., L. Dubrovinsky, et al. (1998). "A new post-stishovite silicon dioxide polymorph with the baddelyite structure (zirconium oxide) in the SNC meteorite sShergotty: evidence for extreme shock pressure." Meteoritics and Planetary Science **33**(4, Suppliment): A45.

El Goresy, A., T. G. Sharp, et al. (1998). "A new very-high-pressure silica mineral in the Shergotty SNC meteorite: implications for shock metamorphism and the Earth's lower mantle." LPSC **XXIX**.

El Goresy, A., B. Wopenka, et al. (1997). "The saga of maskelynite in Shergotty." Meteoritics **32**(Supplement): A38-A39.

Fredriksson, K., P. S. DeCarli, et al. (1963). Shock-induced veins in chondrites. Space Research III, Proc. 3rd Intl. Space Symp. W. Priester. Amsterdam, North-Holland Publ. Co.: 974.

German, V. N., M. A. Podurets, et al. (1973). "Synthesis of a high-density phase of silicon dioxide in shock waves." Soviet Physics JETP **37**(1): 107.

Gillet, P., M. Chen, et al. (2000). "Natural NaAlSi3O8-hollandite in the shocked Sixiangkou meteorite." Science **287**: 1633-1636.

Gratz, A. J., J. Tyburczy, et al. (1988). "Shock metamorphism of deformed quartz." Physics and Chemistry of Minerals **16**: 221-233.

Karki, B. B., M. C. Warren, et al. (1997). "Ab initio studies of high-pressure structural transformations in silica." Physical Review B **55**(6): 3465-3471.

Kingma, K. J., R. E. Cohen, et al. (1995). "Transformation of stishovite to a denser phase at lower-mantle pressures." Nature **374**(16 March): 243-245.

Liu, L. G. (1978). "High=pressure phase transformations of albite, jadeite and nepheline." EPSL **37**: 438-444.

Sekine, T., M. Akaishi, et al. (1987). "Fe2N-type SiO_2 from shocked quartz." Geochimica et Cosmochimica Acta **51**: 379-381.

Sharp, T. G., M. Chen, et al. (1995). "Magnetite inclusions in natural magnesiowüstite from a shocked L6 chondrite." EOS **76**: F564.

Sharp, T. G., M. Chen, et al. (1996). "Microstructures of high-pressure minerals in shocked chondrites: Constraints on the duration of shock." Meteoritics **31**: A127.

Sharp, T. G., M. Chen, et al. (1996). "Microstructures of high-pressure minerals in the Sixiangkou L6 chondrite: Constraints on the duration of shock events in chondrites." LPSC abstracts **XXVII**: 1175-1176.

Sharp, T. G., A. El Goresey, et al. (1998). "Microstructures of shocked silicon dioxide in shergotty: evidence for multiple post-stishovite silicon dioxide polymorphs and extreme pressures." Meteoritics and Planetary Science **33**(4): A144.

Sharp, T. G., A. El Goresy, et al. (1999). "A post-stishovite SiO_2 polymorph in the meteorite Shergotty: implications for impact events." Sciecne **284**(May 21).

Sharp, T. G., A. ElGoresy, et al. (1999). "Very dense silica minerals in the shergotty SNC meteorite: evidence for extreme shock pressures." LPSC **XXX**.

Sharp, T. G., C. M. Lingemann, et al. (1997). "Natural Occurrence of $MgSiO_3$-ilmenite and evidence for $MgSiO_s$-perovskite in a shocked L chondrite." Science **277**: 352-355.

Stöffler, D. (1972). "Deformation and transformation of rock-forming minerals by natural and experimental shock processes." Fortschrift für Mineralogy **49**: 50-113.

Stöffler, D., K. Keil, et al. (1991). "Shock metamorphism of ordinary chondrites." Geochimica Cosmochimica Acta **55**: 3845-3867.

Stöffler, D. and F. Langenhorst (1994). "Shock metamorphism of quartz in nature and experiment: I. Basic observation and theory." Meteoritics **29**: 155-181.

Stöffler, D., R. Ostertag, et al. (1986). "Shock metamorphism and petrography of the Shergotty achondrite." Geochimica et Cosmochimica Acta **50**(6): 889-904.